Multivariable Repetitive-predictive Controllers using Frequency Decomposition

Liuping Wang, Shan Chai, Eric Rogers and Chris T. Freeman.

***Abstract*—Repetitive control is a methodology for the tracking of a periodic reference signal. This paper develops a new approach to repetitive control systems design using receding horizon control with frequency decomposition of the reference signal. Moreover, design and implementation issues for this form of repetitive predictive control are investigated from the perspectives of controller complexity and the effects of measurement noise. The analysis is supported by a simulation study on a multi-input multi-output robot arm where the model has been constructed from measured frequency response data, and experimental results from application to an industrial AC motor.**

I. Introduction

Repetitive control [1] is concerned with the tracking of a periodic reference signal and has many applications, such as robotics [2] and power electronics [3]. This requirement can be formulated by using the internal model control principle [4] (expressed in transfer-function terms) which states that to track a reference signal with zero error the generator polynomial of this signal must be included as part of the controller denominator. In the design of repetitive control systems, the control signal is often generated by a controller that is explicitly described by a transfer-function with appropriate coefficients, see, for example, [1] [5] [6].

If the reference signal for an applications contains multiple frequencies, the repetitive control system will contain all periodic modes, and the number of these is proportional to the period length and inversely proportional to the sampling interval. The result could be a very high order control system, especially under fast sampling, and hence the possibility of numerical sensitivity, noise amplification, sensitivity to modeling errors, and other undesirable problems in practical applications.

An alternative to including all the periodic modes in the repetitive control system is to embed fewer periodic modes at a given time, and when the frequency of the reference signal changes, the coefficients of the controller change accordingly. Previous work [7], [8] has taken this approach, where the frequency components of a given reference signal are analyzed and its reconstruction performed using a frequency sampling filter model, from which the significant frequencies are identified and error analysis is used to justify the selections.

Once the significant frequency components have been selected, the z-transform of the reference signal to be used in design is formed and by the internal model principle the denominator polynomial of this transfer-function must be included in the feedback controller. In this paper, the denominator polynomial model together with the plant description is used to construct an augmented state-space model. Receding horizon control applied to this augmented model results in a feedback controller for the system considered.

For a multi-input multi-output (MIMO) system, the frequency components of all reference signals are analyzed via Fourier analysis and the dominant frequencies are identified based on reconstruction of the reference signals with a pre-defined accuracy. A major reason for considering model predictive control is the ability to impose input, state and output constraints. Using the receding horizon control setting of this paper, input constraints can be imposed in the design and implementation, and the extension to state and output constraints is noted as a future research topic. Moreover, it is shown through a simulation example that the sensitivity of the repetitive-predictive control system in the presence of measurement noise is related to the frequencies included in the design.

This paper is organized as follows. In Section II, the reference trajectory is decomposed using a frequency sampling model to enable selection of the dominant frequencies to be used in controller design. In Section III, the signal generator model is formulated and embedded into a state-space model, which is used for controller design. Section IV, uses the receding horizon control principle to design the repetitive control law. To support the development, the last two sections of the paper give the results of application of the procedure in simulation to a robot arm configured as a two-input and two-output system where the plant model has been constructed from measured frequency response data, and the results from experimental application to a single-input single-output (SISO) industrial AC motor, respectively.

Liuping Wang and Shan Chai are with School of Electrical and Computer Engineering, RMIT University, Victoria 3000 Australia liuping.wang@rmit.edu.au

E. Rogers and C. T. Freeman are with the School of Electronics and Computer Science, University of Southampton, Southampton SO17 1BJ, UK

II. Frequency Decomposition of the Reference Signal

It is shown in this section that the frequency sampling filter model [9] is another representation of a periodic signal. This representation provides insight into the characteristics of the periodic signals and the construction of the signal generator that will be embedded in the structure of repetitive-predictive control system.

A. Frequency Sampling Filter (FSF) Representation of Periodic Signals

Suppose that a periodic reference signal with period T is uniformly sampled with interval Δt to give the corresponding discrete sequence $r(k)$, $k = 0,1,\ldots,M-1$. Here M is defined as $\frac{T}{\Delta t}$, and is assumed to be an odd integer for the reason explained below. We also assume that the periodic reference signal contains no frequency components higher than $\frac{1}{2\Delta t}$. By Fourier analysis, this discrete periodic signal can be uniquely represented by the inverse discrete Fourier transform (DFT) as

$$r(k) = \frac{1}{M}\sum_{i=0}^{M-1} R(e^{j\frac{2\pi i}{M}})e^{j\frac{2\pi ik}{M}}, \tag{1}$$

where the $R(e^{j\frac{2\pi i}{M}})$, $i = 0,1,2,\ldots,M-1$, are the frequency components contained in the periodic signal. Note that the discrete frequencies are at $0, \frac{2\pi}{M}, \frac{4\pi}{M}, \ldots, \frac{(M-1)2\pi}{M}$. For notational simplicity, the fundamental frequency is expressed as $\omega = \frac{2\pi}{M}$. The z-transform of the signal $r(k)$ is defined as

$$R_m(z) = \sum_{k=0}^{M-1} r(k)z^{-k}. \tag{2}$$

Also, by substituting (1) into (2) and interchanging the order of the summation, the z-transform representation of the periodic signal $r(k)$ is obtained as

$$R_m(z) = \sum_{l=-\frac{M-1}{2}}^{\frac{M-1}{2}} R(e^{jl\omega})H^l(z), \tag{3}$$

where $H^l(z)$ is termed the lth frequency sampling filter and has the form

$$\begin{aligned} H^l(z) &= \frac{1}{M}\frac{1-z^{-M}}{1-e^{jl\omega}z^{-1}} \\ &= \frac{1}{M}(1+e^{jl\omega}z^{-1}+\ldots+e^{j(M-1)l\omega}z^{-(M-1)}). \end{aligned}$$

The assumption that M is an odd number is used to include the zero frequency. Moreover, the frequency sampling filters are bandlimited and are centered at $l\omega$. For example, at $z = e^{jl\omega}$, $H^l(z) = 1$, and also (3) can be written in terms of real (denoted Re) and imaginary (denoted Im) parts of the frequency component $R(e^{jl\omega})$ as

$$\begin{aligned} R_m(z) &= \frac{1}{M}\frac{1-z^{-M}}{1-z^{-1}}R(e^{j0}) \\ &+ \sum_{l=1}^{\frac{M-1}{2}} [Re(R(e^{jl\omega}))F_R^l(z) + Im(R(e^{jl\omega}))F_I^l(z)], \end{aligned}$$

where $F_R^l(z)$ and $F_I^l(z)$ are the lth second order filters given by

$$F_R^l(z) = \frac{1}{M}\frac{2(1-cos(l\omega)z^{-1})(1-z^{-M})}{1-2cos(l\omega)z^{-1}+z^{-2}},$$

and

$$F_I^l(z) = \frac{1}{M}\frac{2sin(l\omega)z^{-1}(1-z^{-M})}{1-2cos(l\omega)z^{-1}+z^{-2}},$$

respectively.

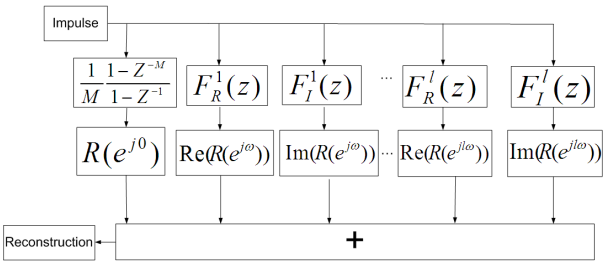

Fig. 1. Block diagram representation of a frequency sampling filter.

The FSF representation of a periodic signal is illustrated in the block diagram of Fig. 1, where each frequency sampling filter is in series with the corresponding weighting of the DFT coefficients, and the outputs of all of them summed to generate the output.

If the filters are assumed to have zero initial conditions, the output is a periodic signal when the input to the discrete-time model is a unit impulse $\delta(k)$, where $\delta(k) = 1$ for $k = 0$ and $\delta(k) = 0$ for $k \neq 0$. Due to the series structure, if the DFT coefficients of some particular frequencies are insignificant, the corresponding coefficients can be neglected and the number of filters required is reduced.

B. The Signal Generator for the Repetitive Controller

Once the significant frequency components in a periodic signal have been obtained, the z-transform of the reference signal $R_m(z)$ is approximated as

$$\begin{aligned} R_m(z) &\approx R_a(z) = \frac{1}{M}\frac{1-z^{-M}}{1-z^{-1}}R(e^{j0}) \\ &+[Re(R(e^{jl_1\omega}))F_R^{l_1}(z) + Im(R(e^{jl_1\omega}))F_I^{l_1}(z)] + \ldots \\ &+[Re(R(e^{jl_n\omega}))F_R^{l_n}(z) + Im(R(e^{jl_n\omega}))F_I^{l_n}(z)], \end{aligned} \tag{4}$$

where $l_1, l_2, \ldots, l_n$ correspond to the indices for the significant frequency components. The denominator of

TABLE I
DFT COEFFICIENTS OF THE REFERENCE SIGNALS

freq. comp.	0	1st	2nd	3rd
R_m^1	167.1810	-195.6558	61.6788	29.1642
R_m^2	679.8660	-115.2289	-146.4782	-12.6684

TABLE II
MEAN SQUARED ERROR OF RECONSTRUCTED SIGNAL

freq. components	0	0-1st	0-2nd	0-3rd
mse of channel 1	0.5344	0.0583	0.0110	0.0004
mse of channel 2	0.4394	0.02743	0.0074	0.0054

the z-transform of the zero frequency filter is $1-z^{-1}$, which is the integrator factor used in discrete-time feedback control systems to, for example, reject constant disturbances or eliminate unknown system bias. Also a pair of filters for an arbitrary frequency, say $l_i\omega$. introduces the term $1-2cos(l_i\omega)z^{-1}+z^{-2}$ into the denominator.

The signal generator polynomial, denoted by $D(z)$, to be included in the repetitive controller is the common denominator of those for the terms in $R_a(z)$ and can be written as

$$D(z) = (1-z^{-1})\prod_{i=1}^{n}(1-2cos(l_i\omega)z^{-1}+z^{-2}). \quad (5)$$

For a MIMO example, the procedure given above generalizes in a natural manner, that is, the above procedure is applied to each entry and then $D(z)$ is formed as the least common denominator of the resulting polynomials.

C. Frequency Decomposition Examples

To illustrate frequency decomposition of periodic reference signals, consider the pair shown over one period ($M = 400$ samples with sampling interval of 0.05 sec) in Figs 2 (a) and (b), respectively. Table I shows the first four DFT coefficients of each signal, which are the dominant components among all the coefficients. For this pair of signals, the imaginary parts of the corresponding DFT coefficients are zero, and (4) can be applied to construct $R_a(z)$ using the coefficients given in Table I. Figures 2(a) and 2(b) compare the reconstructed signal, which is the impulse response of the corresponding model, with the reference signal by selecting different dominant frequency components. The degree of approximation of the reconstructed signal is reflected by the mean square error (mse), as shown in Table II, between reference signal and its reconstruction. These results confirm that for these two example only a few dominant frequency components are required to reconstruct the reference signals.

III. EMBEDDING THE SIGNAL GENERATOR

The repetitive controller is to be designed to follow the reference trajectory and hence, by the internal

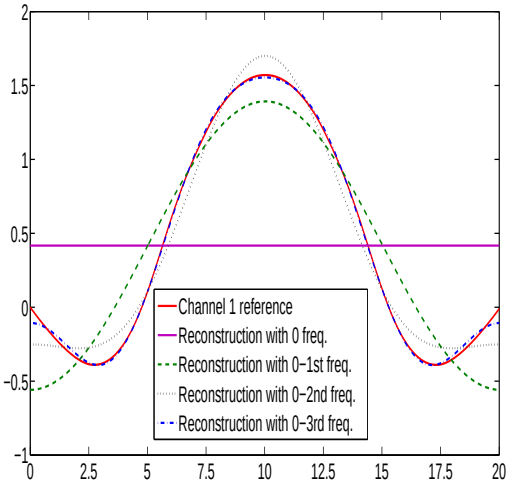

(a) First reference signal reconstruction example

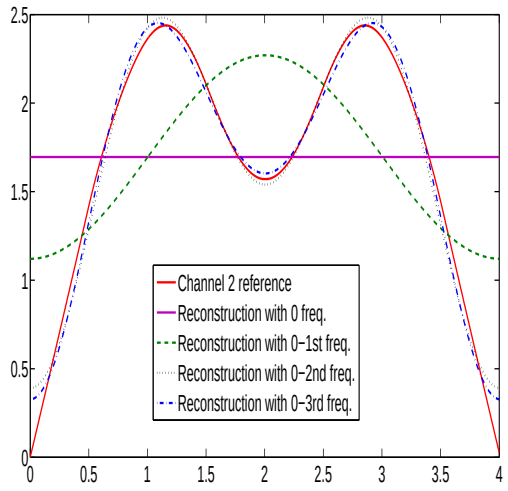

(b) Second reference signal reconstruction example

Fig. 2. Reference signal reconstruction using a limited number of frequencies.

model principle, the required $D(z)$ must be included in the denominator of its z transfer-function description. One way satisfying this requirement is by adding a vector term to the state dynamics in the plant state-space model as detailed next.

Suppose that the plant to be controlled has p inputs and m outputs and consider the state-space model

$$\begin{aligned} x_m(k+1) &= A_m x_m(k) + B_m u(k) + \mu(k), \\ y(k) &= C_m x_m(k), \end{aligned} \quad (6)$$

where $x_m(k)$ is the $n_1 \times 1$ state vector, $u(k)$ is the $p \times 1$ input vector, $y(k)$ is $m \times 1$ output vector, and the $n_1 \times 1$ vector $\mu(k)$ is detailed next.

Given the polynomial $D(z)$ of (5), each entry in $\mu(k)$

is given by the inverse z-transform of $\frac{1}{D(z)}$, and also

$$\begin{aligned} D(z) &= (1-z^{-1})\prod_{i=1}^{n}(1-2cos(l_i\omega)z^{-1}+z^{-2}) \\ &= 1+d_1z^{-1}+d_2z^{-2}+d_3z^{-3}+\ldots+d_\gamma z^{-\gamma}. \end{aligned} \tag{7}$$

In the steady-state, $\mu(k), k \geq k_0$, is described by the following difference equation in the backward shift operator q^{-1}

$$D(q^{-1})\mu(k) = 0, \tag{8}$$

where k_0 corresponds to an initial sampling instant. Also define the following auxiliary variables using the disturbance model

$$x_s(k) = D(q^{-1})x_m(k),\ u_s(k) = D(q^{-1})u(k),$$

where $x_s(k)$ and $u_s(k)$ are the filtered state and control vectors, respectively. Then multiplying the state equation in (6) by $D(q^{-1})$ gives

$$D(q^{-1})x_m(k+1) = A_mD(q^{-1})x_m(k) + B_mD(q^{-1})u(k),$$

or

$$x_s(k+1) = A_mx_s(k) + B_mu_s(k),$$

where (8) has been used. Multiplying output equation in (6) by $D(q^{-1})$ gives

$$\begin{aligned} D(q^{-1})y(k+1) &= C_mx_s(k+1) \\ &= C_mA_mx_s(k) + C_mB_mu_s(k), \end{aligned} \tag{9}$$

and expanding the right-hand side of (9) gives

$$\begin{aligned} y(k+1) = -d_1y(k) - d_2y(k-1) - \ldots - d_{\gamma-1}y(k-\gamma+1) \\ - d_\gamma y(k-\gamma) + C_mA_mx_s(k) + C_mB_mu_s(k). \end{aligned}$$

Introduce the state vector

$$x(k) = \left[\begin{array}{ccccc} x_s(k)^T & y(k)^T & y(k-1)^T & \ldots & y(k-\gamma)^T \end{array}\right]^T,$$

to obtain the following augmented model of the plant and disturbance to be used in controller design

$$\begin{aligned} x(k+1) &= Ax(k) + Bu_s(k) \\ y(k) &= Cx(k) \end{aligned} \tag{10}$$

Also introduce the matrix

$$A_d = \left[\begin{array}{ccccc} -d_1I & -d_2I & \ldots & -d_{\gamma-1}I & -d_\gamma I \\ 0 & I & 0 & \ldots & 0 \\ \vdots & \ddots & \ddots & \ddots & \vdots \\ 0 & 0 & \ldots & I & 0 \end{array}\right].$$

where from this point onwards 0 and I denote the zero and identity matrices, respectively, with compatible dimensions. Then

$$A = \left[\begin{array}{cc} A_m & 0 \\ \hat{C} & A_d \end{array}\right]$$

where

$$\hat{C} = \left[\begin{array}{c} C_mA_m \\ 0 \end{array}\right]$$

The characteristic equation of the state matrix in (10) is

$$\det(zI-A) = \det(zI-A_m)\det(zI-A_d) = 0$$

and the roots of this equation are the union of the poles of the original plant model and those of $D(z)$.

IV. Discrete-time Repetitive-predictive Control

Given the augmented state-space model, the next task is to synthesize the filtered control signal $u_s(k)$ using model predictive control, which is a well established area, see for example, [10], [11], and [12]. Hence only the main steps required for the current task are given.

Consider sampling instant k_i, $k_i > 0$, and assume that the state vector $x(k_i)$, and hence current plant information, is available through measurement. Moreover, the future control trajectory can be written in vector form as

$$U_s = \left[\begin{array}{cccc} u_s(k_i) & u_s(k_i+1) & \ldots & u_s(k_i+N_c-1) \end{array}\right]^T,$$

where N_c is the control horizon dictating the number of parameters used to capture the future control trajectory. Given $x(k_i)$, the future state vectors are predicted for N_p samples, where N_p is termed the prediction horizon and it is assumed that $N_c \leq N_p$. Let the predicted state vectors be denoted by $x(k_i+j|k_i)$, $1 \leq j \leq N_p$, and introduce, for computational purposes,

$$X = \left[\begin{array}{ccc} x(k_i+1 \mid k_i)^T & \ldots & x(k_i+N_p \mid k_i)^T \end{array}\right]^T.$$

In this design, the control horizon is selected to be less than the prediction horizon to reduce the computational load. It is assumed that after N_c samples the filtered control signal $u_s(k_i+k)$ is zero for all future samples ($k \geq N_c$). Using the augmented state-space model (10), the future state vectors are computed sequentially using U_s as

$$X = F_xx(k_i) + \Phi_sU_s, \tag{11}$$

where

$$F_x = \left[\begin{array}{c} A \\ A^2 \\ \vdots \\ A^{N_p} \end{array}\right] \Phi_s = \left[\begin{array}{cccc} B & 0 & .. & 0 \\ AB & B & .. & 0 \\ A^2B & AB & .. & 0 \\ \vdots & \vdots & .. & \vdots \\ A^{N_p-1}B & A^{N_p-2}B & .. & A^{N_p-N_c}B \end{array}\right],$$

The design criterion for the repetitive-predictive controller is to find the control parameter vector U_s such that the following cost function is minimized

$$J = X^T\bar{Q}X + U_s^T\bar{R}U_s,$$

where $\bar{Q}$ is a block diagonal matrix of the form QI, where Q is a symmetric positive semi-definite matrix (with (Q,A) detectable), and $\bar{R}$ is of the form RI, where R is a symmetric positive definite matrix. Substituting (11) into the cost function gives

$$J = U_s^T(\Phi_s^T\bar{Q}\Phi_s + \bar{R})U_s + 2U_s^T\Phi_s^T\bar{Q}F_x x(k_i) + x(k_i)^T F_x^T Q F_x x(k_i). \quad (12)$$

In the absence of constraints, the optimal control vector is

$$U_s = -(\Phi_s^T\bar{Q}\Phi_s + \bar{R})^{-1}\Phi_s^T\bar{Q}F_x x(k_i). \quad (13)$$

Using receding horizon control, only the components in U_s corresponding to $u_s(k_i)$ are used and the actual control signal applied to the plant is computed using

$$D(q^{-1})u(k_i) = u_s(k_i),$$

or, using (7) and noting that the leading coefficient in the polynomial $D(q^{-1})$ is unity,

$$u(k_i) = u_s(k_i) - d_1u(k_i-1) - \ldots - d_\gamma u(k_i-\gamma) \quad (14)$$

where both the current optimal control $u_s(k_i)$ and past values are used.

When the repetitive-predictive controller is used for disturbance rejection, the control objective is to maintain the plant in steady-state operation, and the filtered state vector $x_s(k_i)$ has zero steady-state whilst the steady-state of the plant output is a constant (vector in the MIMO case). When the repetitive-predictive controller is used for tracking a periodic input signal, the reference signal will enter the computation through the augmented output variables. Note that the state vector $x(k_i)$ contains the filtered state vector $x_s(k_i)$, and the output $y(k_i)$, $y(k_i-1)$, …, $y(k_i-\gamma)$, and hence at the sampling instant k_i, the feedback errors are

$$[y(k_i)-r(k_i)\ \ldots\ y(k_i-\gamma+1)-r(k_i-\gamma+1)]^T = [e(k_i)\ e(k_i-1)\ \ldots\ e(k_i-\gamma+1)]^T.$$

These error signals will replace the original output elements in $x(k_i)$ to form the state vector for use in (11).

The repetitive control law given by (13) and (14) is in the form of state feedback control. The closed-loop performance of the repetitive control system is determined by the choice of the weighting matrices Q and R. In common with other repetitive control systems designed using transfer-function models [1] [5] [6], this control system can be applied to track periodic reference signals and reject periodic disturbances.

Model predictive control enables the placing of constraints on the plant input and output variables. As a first step in this respect for the repetitive-predictive controller developed in this paper the application of input constraints is considered, where the constrained control system minimizes the cost function J (12) in real-time subject to the constraints imposed. In particular, we consider control amplitude constraints imposed at the sampling instant k written in the form of a set of linear inequalities

$$u^{min} \le u(k) \le u^{max}, \quad (15)$$

where u^{min} and u^{max} are $q \times 1$ data vectors containing the required lower and upper limits of the control amplitude for each input signal, respectively. Also, the incremental changes in the control signal ($\Delta u(k) = u(k) - u(k-1)$) are limited in practical applications. Consequently in the final form of the constrained repetitive-predictive control problem, the constraints are written in the form

$$\Delta u^{min} \le \Delta u(k) \le \Delta u^{max}. \quad (16)$$

The repetitive-predictive controller is then obtained by minimizing the cost function (12) subject to (15) and (16) by direct application of quadratic programming algorithms in, for example, [13] and [12].

V. Design Examples

A. A Simulation Study with Constrained Control

This case study is for a two-input and two-output model obtained from frequency domain tests on anthropomorphic robotic arm undertaking a pick and place operation. The robot arm has been configured to perform 'pick and place' tasks in a horizontal plane using two joints and is shown in Fig. 3. Its end-effector travels between the pick and place locations in a straight line using joint reference trajectories which minimize the end-effector acceleration. Having reached the place location, the robot then returns back to the starting location.

Repetitive control is often applied in what is termed 'plug-in' mode, that is, a stabilizing control law is first applied to the plant and then the repetitive control is applied to the resulting system. In this example, position and velocity control loops have been implemented around each joint to provide the first layer of control system and the control scheme operates at 20 Hz. The overall system model has been identified by combining experimentally-derived models of its constituent components as described by the transfer-function matrix description (17).

Using the reference trajectories given in Fig. 2 and (7), a repetitive-predictive controller has been designed, where the weighting matrix Q is selected such that the sum of squared output errors is used in the cost function, i.e., all entries in this matrix are zeros except for a 2×2 identity matrix corresponding to the outputs; the weighting matrix R is the identity matrix; the prediction horizon is 30, the control horizon for

$$\begin{bmatrix} y_1 \\ y_2 \end{bmatrix} = \begin{bmatrix} G_{11}G_{12} \\ G_{21}G_{22} \end{bmatrix} \begin{bmatrix} u_1 \\ u_2 \end{bmatrix}, \tag{17}$$

where

$$G_{11}(s) = \frac{0.16s^9 + 14.51s^8 + 578.2s^7 + 1.392e4s^6 + 2.26e5s^5 + 2.58e6s^4 + 2.09e7s^3 + 1.17e8s^2 + 4.21e8s + 7.6e8}{5.25e - 5s^{12} + 0.01463s^{11} + 0.91s^{10} + 31.2s^9 + 714.1s^8 + 1.19e4s^7 + 1.45e5s^6 + 1.4e6s^5 + 1.01e7s^4 + 5.7e7s^3 + 2.3e8s^2 + 5.9e8s + 7.6e8},$$

$$G_{12}(s) = \frac{-0.022s^7 - 3.24s^6 - 88.3s^5 - 1347s^4 - 1.06e4s^3 - 4.52e4s^2}{5.25e - 5s^10 + 0.014s^9 + 0.72s^8 + 20s^7 + 363s^6 + 4645s^5 + 4.3e4s^4 + 2.9e005s^3 + 1.4e6s^2 + 4.18e6s + 6.323e6},$$

$$G_{21}(s) = \frac{-0.16s^7 - 8.7s^6 - 194s^5 - 2498s^4 - 1.78e4s^3 - 6.64e4s^2}{5.25e - 5s^{10} + 0.014s^9 + 0.67s^8 + 17.9s^7 + 316s^6 + 3963s^5 + 3.6e4s^4 + 2.42e5s^3 + 1.1e6s^2 + 3.5e6s + 5.3e6},$$

$$G_{22}(s) = \frac{0.027s^9 + 4.95s^8 + 264s^7 + 7394s^6 + 1.3e5s^5 + 1.69e6s^4 + 1.5e7s^3 + 9.4e7s^2 + 3.8e8s + 7.6e8}{5.25e - 5s^{12} + 0.014s^{11} + 0.9s^{10} + 31s^9 + 714.1s^8 + 1.19e4s^7 + 1.48e5s^6 + 1.4e6s^5 + 1.04e7s^4 + 5.7e7s^3 + 2.3e8s^2 + 5.9e8s + 7.6e8}.$$

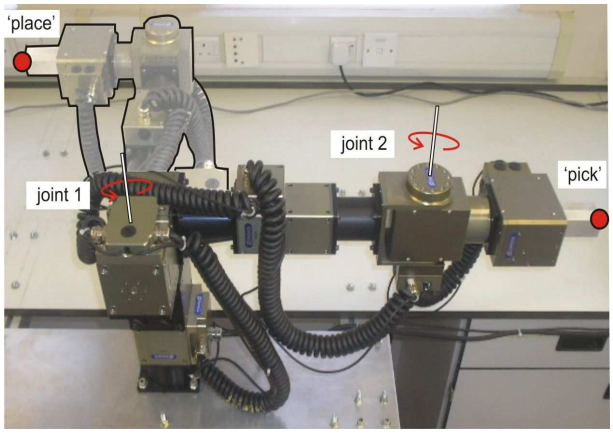

Fig. 3. Robot arm with th3e pick and place locations shown.

both inputs is selected as $N_c = 6$. The constraints for the operation of the robot arm are specified as

$$-1 \le u_1(k) \le 3.8 \qquad -3.8 \le u_2(k) \le 3$$
$$-0.5 \le \Delta u_1 \le 0.5 \qquad -0.5 \le \Delta u_2 \le 0.5.$$

In the simulation studies, all initial conditions are set to zero, and at $t = 2.5$ secs, two step input disturbances enter the system, where the first of these has amplitude 0.5 and the second -0.8. The quadratic programming algorithm in [12] was used to solve the constrained control problem.

Figure 4 shows comparisons of the closed-loop outputs with the reference signals, Fig. 5 the control signals used to generate the outputs of the repetitive-predictive control system, and Fig. 6 the incremental control signals, respectively. In this case the repetitive control system has produced the outputs which follow the reference signals with all constraints satisfied. The sum of the squared error between the reference signal r_1 and the output y_1 is 0.59 and between r_2 and y_2 is 0.9.

To assess the sensitivity of the controller structure to measurement noise, two independent white noise signals with variance 0.05 were added to the system outputs. The first four frequencies are embedded in the controller. Figure 7 shows a comparison of the

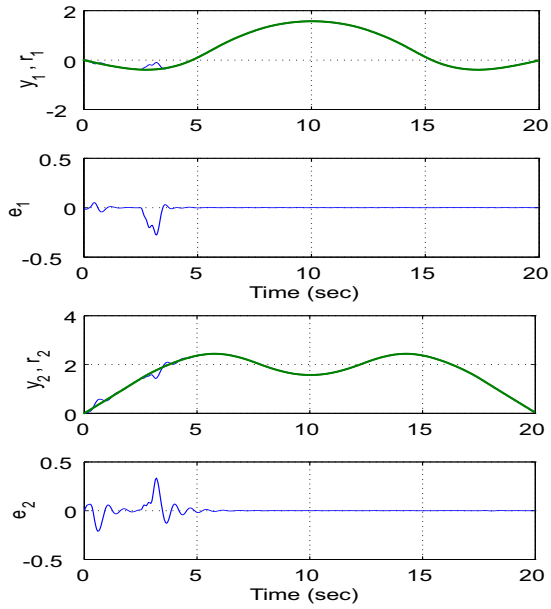

Fig. 4. Comparison between outputs (y_1, y_2), references (r_1, r_2) and errors (e_1, e_2).

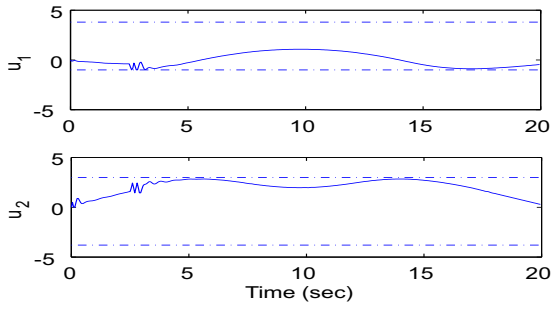

Fig. 5. Control signals. The top plot is u_1 and the bottom u_2.

closed-loop outputs and reference signals. In this case, the measurement noise has been amplified and clearly affects the closed-loop performance. The mean squared error between the reference signal r_1 and the output y_1 is 0.5192 and between r_2 and y_2 is 1.429. Both values are much larger than the mean squared errors resulted from the approximation shown in Table II, which were 0.0004 and 0.0054, respectively. To demonstrate that

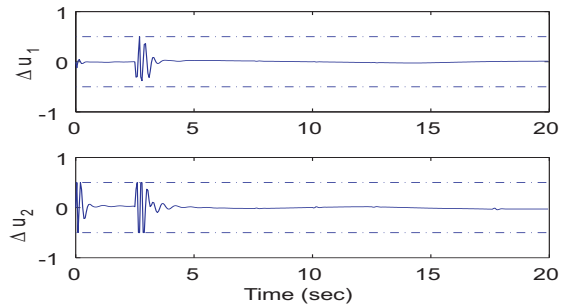

Fig. 6. Incremental control signals. The top is Δu_1 and the bottom Δu_2.

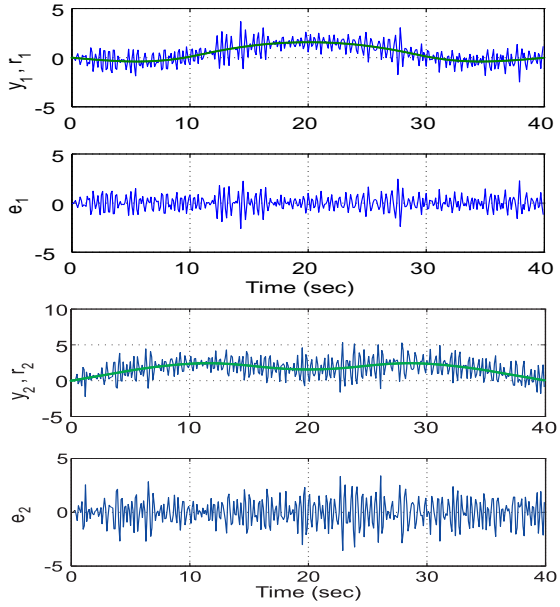

Fig. 7. Comparison between output and reference. The first two give y_1 and r_1, and e_1, respectively, and the bottom two y_2 and r_2, and e_2 respectively.

this sensitivity is related to the number of frequencies embedded in the repetitive-predictive controller, a reduced order disturbance model is used, where

$$D(z) = (1-z^{-1})(1-2cos(2\pi/400)z^{-1}+z^{-2}).$$

Given this disturbance model, Fig. 8 shows the closed-loop output response for y_1 and the error signal. The mean squared error between the reference signal r_1 and y_1 is 0.0185 and between the reference r_2 and y_2 is 0.0342.

B. Experimental Verification

One general application area for repetitive control is electric motors, such as a Permanent Magnet Synchronous Motor (PMSM), a brushless DC motor (BLDC), and the induction motor (IM). In these a repetitive task can be performed by position control of the motor with a periodic reference trajectory. As a first experimental validation of the new design in this

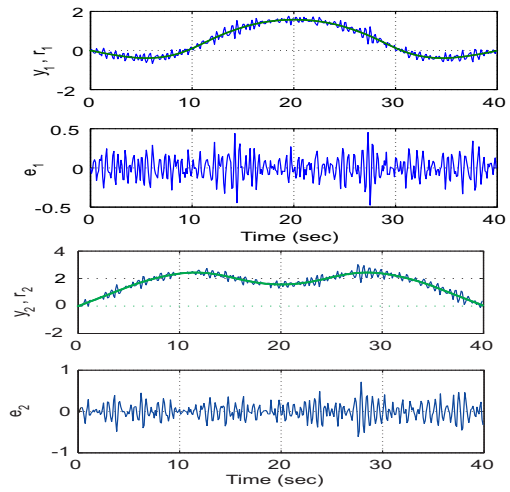

Fig. 8. Comparison between output and reference. The first two give y_1 and r_1, and e_1, respectively, and the bottom two y_2 and r_2, and e_2 respectively.

paper, it has been implemented on a laboratory test-bed for the purpose of controlling a PMSM. A schematic of the control system for the testbed is shown in Fig. 9. The drive of a PMSM consists of an Insulated-Gate Bipolar Transistor (IGBT) inverter controlled by Sinusoidal Pulse Width Modulation (SPWM). The three-phase currents are measured by the current sensors and transformed into a d-q axis representation by abc/dq transformation.

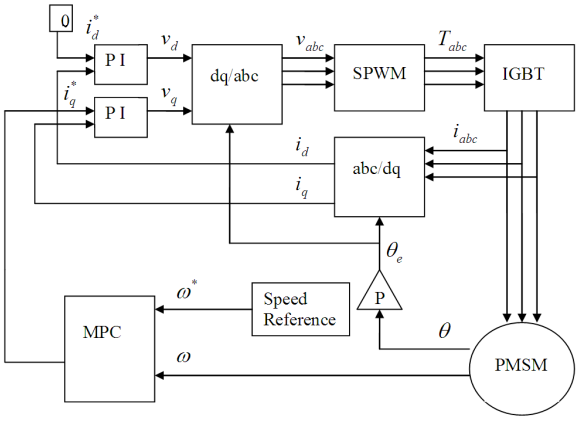

Fig. 9. Schematic of Repetitive-predictive control of a PMSM motor

The current loop control is Proportional and Integral (PI), and by maintaining the i_d component of feedback current at zero, the algorithm can utilize the linear mechanical model of PMSM to optimize the i_q component using

$$\begin{bmatrix} \dot{\omega}_r \\ \dot{\theta}_r \end{bmatrix} = \begin{bmatrix} -\frac{B}{J} & 0 \\ 1 & 0 \end{bmatrix} \begin{bmatrix} \omega_r \\ \theta_r \end{bmatrix} + \begin{bmatrix} \frac{1}{J} \\ 0 \end{bmatrix} T_e,$$

$$T_e = K_t i_q, \quad \omega_e = P\omega_r,$$

where the load torque T_L is assumed to be zero, $J(=0.94Kg.cm^2)$ is the moment of inertia, $B(=0.0012)$ is the viscous coefficient, $K_t(=0.51)$ is the torque constant, $P(=2)$ is the number of pair of poles and θ_r and θ_e represent the mechanical and electrical angles of the rotor position, ω_r and ω_e are the mechanical and electrical velocities of the rotor, respectively.

A periodic signal $\theta_r^* = 3.14 + 3sin(\frac{2\pi}{6}t)$ with a period of 6 seconds was used as the reference signal of position and the state variables in this case are rotor speed ω_r and angle θ_r respectively, which can be directly measured and calculated from encoder feedback. The model was developed in MATLAB Simulink and downloaded to a XPC target kernel on a target PC with a sampling time of $150(\mu s)$. Figure 10 shows the tracking performance of the repetitive-predictive controller with two dominant frequency components included and the required control signal (the q axis current command).

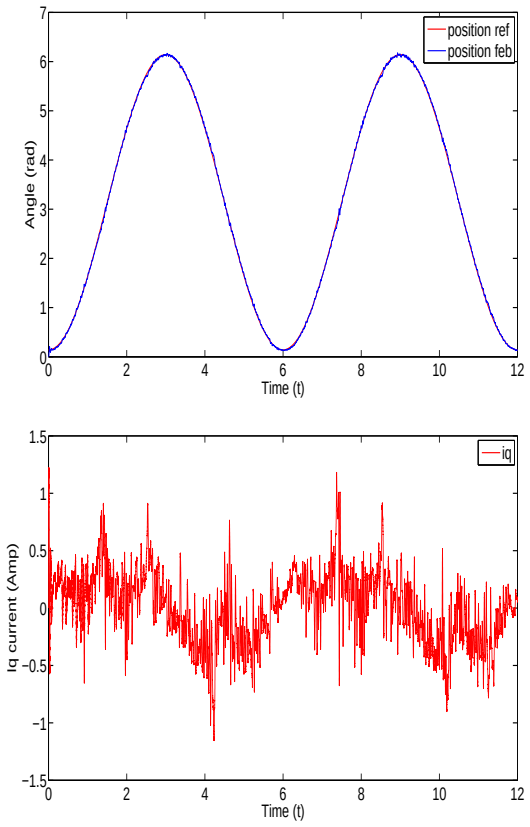

Fig. 10. Controlled system responses for the PMSM motor. The top plot gives the reference and output, respectively, and the bottom the control signal required.

VI. Conclusions

This paper has developed a repetitive-predictive controller for multivariable systems with structure determination. Firstly, a set of candidate frequencies is obtained through the frequency analysis of the reference trajectories; secondly, the set of candidate frequencies is examined in terms of their effect on the improvement of tracking performance and amplification of measurement noise. A case study on a two-input two-output robot arm has demonstrated that including fewer dominant frequencies can provide highly accurate tracking ability without greatly increasing system order and amplification of measurement noise. In a second example, the algorithm has been applied to a PMSM motor giving measured results that confirm that simulation-based performance can be achieved in physical application.

A key strength of model predictive control is the ability to include constraints and there is a clear need to extend this feature to the repetitive-predictive controller developed in this paper. As a first step in solving this problem, it has been demonstrated that constraints on the control signal can be included and the resulting design problem solved by well known techniques. This area requires further research on, for example, the inclusion of state and output constraints.

References

[1] S. Hara, Y. Yamamoto, T. Omata, and M. Nakano, “Repetitive control system: a new type servo system for periodic exogenous signals,” *IEEE Transactions on Automatic Control*, vol. 33, no. 7, pp. 659–668, 1988.

[2] K. Kaneko and R. Horowitz, “Repetitive and adaptive control of robot manipulators with velocity estimation,” *IEEE Tranactions on Robotics Automation*, vol. 13, no. 2, pp. 204217, 1997.

[3] X. H. Wu, S. K. Panda, and J. X. Xu, ”Design of a plug-in repetitive control scheme for eliminating supply-side current harmonics of three-phase PWM boost rectifiers under generalized supply voltage conditions”, *IEEE Transactions on Power Electronics*, vol. 25, no. 7, pp. 1800=-1810, 2010.

[4] B. A. Francis and W. M. Wonham, “The internal model principle of control theory,” *Automatica*, vol. 5, no. 12, pp. 457–465, 1976.

[5] G. Hillerstrom, “Adaptive suppression of vibrations - a repetitive control approach,” *IEEE Transactions on Control Systems Technology*, vol. 4, no. 1, pp. 72 –78, 1996.

[6] D. H. Owens, L. M. Li and S. P. Banks, “Multi-periodic repetitive control system: a Lyapunov stability analysis for MIMO systems,” *International Journal of Control*, vol. 77, pp. 504–515, 2004.

[7] L. Wang, P. Gawthrop, D. H. Owens, and E. Rogers, “Switched linear predictive controllers for periodic exogenous signals,” *International Journal of Control*, vol. 83, no. 4, pp. 848–861, 2010.

[8] L. Wang, S. Chai, and E. Rogers, “Predictive repetitive control based on frequency decomposition,” in Proc *American Control Conference 2010, Baltimore, USA*, July 2010, pp. 4277–4282.

[9] R. R. Bitmead and B. D. O. Anderson, “Adaptive frequency sampling filters,” *IEEE Transactions on Circuits and Systems*, vol. 28, no. 6, pp. 524 – 534, 1981.

[10] J. M. Maciejowski, *Predictive Control with Constraints*, Pearson Education Limited, 2002.

[11] D. Mayne, J. Rawlings, C. Rao, and P. Scokaert. “ Constrained model predictive control: stability and optimality,” *Automatica*, Vol. 36, pp. 789–814, 2000.

[12] L. Wang, *Model Predictive Control System Design and Implementation Using MATLAB*, 1st ed. Springer London, 2009.

[13] D. G. Luenberger, *Linear and Nonlinear Programming*. Second edition, Addison-Wesley Publishing Company, 1984.